12th IFAC International Symposium on
Advanced Control of Chemical Processes
July 14-17, 2024. Toronto, Canada

Optimal control of photobioreactor accounting for photoinhibition and photoacclimation

J. Ignacio Fierro U. * **Benoît Chachuat** ** **Olivier Bernard** *,***

* *Université Côte d'Azur (UCA), Inria, INRAE, CNRS, Sorbonne Université, Biocore Team, 06902 Sophia Antipolis, Valbonne, France, (e-mail: joel-ignacio.fierro-ulloa@inria.fr)*
** *The Sargent Centre for Process Systems Engineering, Department of Chemical Engineering, Imperial College London, London SW7 2AZ, United Kingdom., (e-mail: b.chachuat@imperial.ac.uk)*
*** *Laboratoire d'Océanographie de Villefranche-sur-Mer, Sorbonne Université CNRS UMR 7093, Vilefranche-sur-Mer, France, (e-mail: olivier.bernard@inria.fr)*

Abstract: The industrial cultivation of microalgae has increased substantially over the past two decades. These microorganisms have the ability to adapt their photosynthetic pigments in response to the amount of light they experience. Herein, we investigate a dynamic model that describes pigment adaptation and its effect on microalgal productivity in a photobioreactor where light is shone onto the surface and attenuated as it traverses the culture medium. We consider two controls – the light irradiance and the dilution rate of the photobioreactor under continuous operation and constant volume – and analyze strategies for maximal production of microalgal biomass using Pontryagin's maximum principle. We also conduct a numerical investigation of turnpike properties in this context and discuss how self-shading within the culture could be exploited to increase productivity.

Keywords: Pontryagin's maximum principle; Turnpike; Non-linear systems; Optimal control.

1. INTRODUCTION

Microalgae are microorganisms that convert carbon dioxide (CO_2) into biomass via photosynthesis. They are increasingly used for food and feed production, and in the cosmetic or pharmaceutical industries [Vázquez-Romero et al. 2022]. A wide range of phenomena affects the metabolism and growth of microalgae and, ultimately, their productivity. The main focus in this paper is on photoinhibition and photoacclimation, the combined effect of which has not been studied extensively thus far. Photoinhibition is triggered by an excess of light, causing damage to key photosynthetic proteins and thereby affecting cell growth. Photoacclimation, on the other hand, is a protective mechanism to mitigate photoinhibition through adjusting the amount of cellular pigments in response to light intensity variations. These phenomena take place on different timescales [Hartmann et al. 2014, Bernardi et al. 2017]. While photoinhibition acts on a timescale of minutes, photoacclimation takes place on a timescale of days which is slower than the growth dynamics.

An optimal control problem for maximizing microalgae production was recently studied by Fierro U. et al. [2023], with a focus on the fast dynamics of photoinhibition in a culture medium where the cells experience a gradient of light along their advection. Herein, the objective is to complement this work through bringing the slower photoacclimation dynamics into the analysis. When both the light and the dilution rate can be controlled, a key question is how to avoid loss of productivity in early stages when the culture density is low. This loss is even more severe when an innoculum pre-acclimated at low light is used, for instance a high density inoculum where light seldom penetrates. This leads to a new control problem that we formalize and then analyze to understand how photoacclimation can impact the optimal strategy.

The rest of the paper is organized as follows. Section 2 introduces the dynamic model of biomass growth in the photobioreactor, based on a model by Nikolaou et al. [2016] that integrates both photoinhibition and photoacclimation. Section 3 formulates the optimal control problem, before conducting a formal analysis based on Pontryagin's maximum principle in Section 4. A numerical investigation is conducted in Section 5 to validate and complement the theoretical results. Finally, Section 6 discusses the main insights, in particular the role played by both timescales and the benefits of self-shading on process productivity.

2. DYNAMIC MODEL FORMULATION

We consider a planar photobioreactor operated in continuous mode and illuminated by shining an artificial light onto

⋆ This project has received funding from the Digitalgaesation project within the European Union's Horizon 2020 research and innovation program under the Marie Skłodowska-Curie grant agreement No. 955520

the plane. The biomass concentration, x [$g_C\,L^{-1}$] follows the dynamics:

$$\dot{x} = \mu x - Rx - Dx, \tag{1}$$

where μ [s^{-1}] is the specific gross growth rate, R [s^{-1}] the specific maintenance rate [Blanken et al. 2016], and D [s^{-1}] the dilution rate of the reactor (ratio between the feed rate and the volume of the reactor).

The photobioreactor is illuminated with a light irradiance I [$\mu mol\,m^{-2}s^{-1}$]. This irradiance is attenuated by the biomass concentration x and the amount of chlorophyll $x\theta$, where the chlorophyll quota θ [$g_{Chl}\,g_C^{-1}$] is the amount of chlorophyll per unit of biomass. The average light that the microalgae perceive along their advection in the reactor can be approximated using the Beer-Lambert law: [1]

$$\bar{I}(I, x, I_g) = I\frac{1 - e^{-(E_C + E_{Chl}\theta)xL}}{(E_C + E_{Chl}\theta)xL}, \tag{3}$$

where L [m] is the depth of the photobioreactor (the distance between the illuminated surface and the bottom), E_{Chl} [$g_{Chl}^{-1}\,m^{-1}L$] and E_C [$g_C^{-1}m^{-1}L$] are constants that account for light absorption by the pigments and the biomass, respectively.

The chlorophyll content in microalgae, and more generally their pigment composition, changes in response to variations in the light irradiance. In the model developed by Nikolaou et al. [2016], the chlorophyll quota θ depends on the *growth irradiance* I_g [$\mu mol\,m^{-2}s^{-1}$], which corresponds to the light at which the microalgae are acclimated:

$$\theta(I_g) = \psi\frac{k_I}{I_g + k_I}, \tag{4}$$

with parameters ψ [$g_{Chl}\,g_C^{-1}$] and k_I [$\mu mol\,m^{-2}s^{-1}$]. The dynamics of the growth irradiance I_g are given by:

$$\dot{I}_g = \delta\mu(\bar{I} - I_g), \tag{5}$$

where δ [–] is a scaling constant, and the specific growth rate μ depends on the average perceived light $\bar{I}$ according to the reduced Han model [Han 2002, Hartmann et al. 2014, Fierro Ulloa et al. 2023]:

$$\mu(I, x, I_g) = \frac{K\sigma\bar{I}}{1 + \tau\sigma\bar{I} + \frac{k_d}{k_r}\tau(\sigma\bar{I})^2}, \tag{6}$$

with K [–] the growth rate coefficient, σ [$m^2\mu mol^{-1}$] the effective cross-section, τ [s] the turnover time (time needed to harvest one photon), and k_d [–] and k_r [s^{-1}] the damage and repair rates, respectively. The maximal growth rate,

$$\mu_{max} = \frac{K}{2\sqrt{\frac{k_d}{k_r}}\tau + \tau}, \tag{7}$$

is achieved under the following condition:

$$\sigma\bar{I} = \frac{1}{\sqrt{\frac{k_d}{k_r}}\tau}. \tag{8}$$

Finally, the dependence between the effective cross-section and the chlorophyll quota is assumed to follow a power law relationship with constants β and κ [Nikolaou et al. 2016]:

$$\sigma = \beta\theta^{\kappa}. \tag{9}$$

[1] For simplicity, we denote

$$\varepsilon(x, I_g) = \frac{1 - e^{-(E_C + E_{Chl}\theta)xL}}{(E_C + E_{Chl}\theta)xL}, \tag{2}$$

as the average attenuation factor. In particular, we have $\bar{I} = I\varepsilon$.

3. OPTIMAL CONTROL PROBLEM STATEMENT

The goal is to speed up the reactor's start-up phase or, equivalently, to maximize the total biomass production over the start-up horizon $[0, T_f]$, defined as:

$$J_{T_f}(D, I) = \int_0^{T_f} x(t)D(t)dt\,. \tag{10}$$

The controls are the dilution rate D and the artificial irradiance I, within the following sets of admissible controls:

$$\begin{aligned}\mathcal{D} &:= \{D : [0, +\infty) \to [0, D_{max}]\,; \quad D(\cdot) \in \mathcal{L}^\infty_{loc}(\mathbb{R}_+)\},\\ \mathcal{I} &:= \{I : [0, +\infty) \to [0, I_{max}]\,; \quad I(\cdot) \in \mathcal{L}^\infty_{loc}(\mathbb{R}_+)\},\end{aligned} \tag{11}$$

where $\mathcal{L}^\infty_{loc}(\mathbb{R}_+)$ denotes the set of locally integrable functions on every compact set in $[0, \infty)$. In particular, the upper bounds D_{max} and I_{max} on the controls are assumed to be large enough to drive biomass washout—e.g., $D_{max} > \mu_{max}$ with μ_{max} as defined in Eqn. (7)—and photoinhibition, respectively.

The resulting optimal control problem can be stated as:

$$\begin{aligned}\max_{\substack{D\in\mathcal{D},\\ I\in\mathcal{I}}} \quad & J_{[0,T_f]}(D, I) = \int_0^{T_f} x(t)D(t)dt,\\ \text{s.t.} \quad & \dot{x} = \mu(I, x, I_g)x - Dx - Rx,\\ & \dot{I}_g = \delta\,\mu(I, x, I_g)\left[\bar{I}(I, x, I_g) - I_g\right],\\ & x(0), I_g(0) \text{ given.}\end{aligned} \tag{OCP}$$

4. FORMAL ANALYSIS

To apply Pontryagin's maximum principle (PMP) [Clarke 2013, Hocking 1991] to the optimal control problem (OCP), we define the Hamiltonian function H as:

$$H(x, I_g, D, I, \lambda_x, \lambda_g) := \lambda_x(\mu - R - D)x + \delta\lambda_g\mu(\bar{I} - I_g) + xD\,. \tag{12}$$

The dynamics of the co-states λ_x and λ_g are given by:

$$\begin{aligned}\dot{\lambda}_g &= -\lambda_x\frac{\partial\mu}{\partial I_g}x - \delta\lambda_g\left(\frac{\partial\mu}{\partial I_g}(\bar{I} - I_g) + \mu\left(\frac{\partial\bar{I}}{\partial I_g} - 1\right)\right)\\ \dot{\lambda}_x &= -\lambda_x\left(\frac{\partial\mu}{\partial x}x + \mu - R - D\right)\\ &\quad - \delta\lambda_g\left(\frac{\partial\mu}{\partial x}(\bar{I} - I_g) + \mu\frac{\partial\bar{I}}{\partial x}\right) - D.\end{aligned} \tag{13}$$

Since the terminal states are free, the terminal co-states are given by:

$$\lambda_x(T_f) = \lambda_g(T_f) = 0. \tag{14}$$

The optimal control trajectories $D^*(t), I^*(t)$ are those maximizing the Hamiltonian function for almost all $t \in [0, T_f]$:

$$(D^*(t), I^*(t)) \in \underset{\substack{D\in[0,D_{max}],\\ I\in[0,I_{max}]}}{\text{argmax}}\, H(x^*(t), I_g^*(t), D, I, \lambda_x^*(t), \lambda_g^*(t))\,. \tag{15}$$

Based on condition (15), the optimal dilution rate can take three different values depending on the value of the co-state λ_x, as summarized in Proposition 1 below.

Proposition 1. *For almost all $t \in [0, T_f]$, the optimal control D^* satisfies*

$$D^*(t) = \begin{cases} 0, & \text{if } \lambda_x > 1, \\ D_{\max}, & \text{if } \lambda_x < 1, \\ D_{\text{sing}}(t), & \text{if } \lambda_x(t) = 1, \end{cases} \tag{16}$$

where D_{sing} is a singular arc.

Likewise, the optimal irradiance I^* is a solution to the following problem almost everywhere:

$$I^*(t) \in \underset{I\in[0,I_{\max}]}{\operatorname{argmax}}\ \phi(I) \coloneqq \lambda_x \mu x + \delta\lambda_{\text{g}}\mu(\bar{I} - I_{\text{g}}). \tag{17}$$

The KKT conditions for this problem are given by:

$$\frac{\partial \phi(I)}{\partial I} - \nu = 0, \tag{18}$$

$$\nu(I_{\max} - I) = 0, \tag{19}$$

$$\nu \geq 0. \tag{20}$$

In particular, the stationarity condition (18) expands as:

$$\lambda_x x \frac{\partial \mu}{\partial \bar{I}}\frac{\partial \bar{I}}{\partial I} + \delta\lambda_{\text{g}}\frac{\partial \mu}{\partial \bar{I}}\frac{\partial \bar{I}}{\partial I}(\bar{I} - I_{\text{g}}) + \delta\lambda_{\text{g}}\mu\frac{\partial \bar{I}}{\partial I} - \nu = 0. \tag{21}$$

Since $\frac{\partial \bar{I}}{\partial I} \geq 0$, it follows from the dual feasibility condition (20) that

$$\Psi \coloneqq \lambda_x x \frac{\partial \mu}{\partial \bar{I}} + \delta\lambda_{\text{g}}\left[\frac{\partial \mu}{\partial \bar{I}}(\bar{I} - I_{\text{g}}) + \mu\right] \geq 0. \tag{22}$$

The switching function Ψ is such that $I^*(t) = I_{\max}$ whenever $\Psi > 0$. Next, we seek an expression of $I^*(t)$ when $\Psi = 0$:

$$\lambda_x x \frac{\partial \mu}{\partial \bar{I}} + \delta\lambda_{\text{g}}\left[\frac{\partial \mu}{\partial \bar{I}}(\bar{I} - I_{\text{g}}) + \mu\right] = 0. \tag{23}$$

In the case that $\delta\lambda_{\text{g}} = 0$, the previous condition simplifies to:

$$\lambda_x x \frac{\partial \mu}{\partial \bar{I}} = 0, \tag{24}$$

then dismissing the case $\lambda_x = 0$, the optimal solution corresponds to:

$$\sigma\bar{I}^* = \frac{1}{\sqrt{\frac{k_d}{k_r}\tau}}. \tag{25}$$

In the other case that $\delta\lambda_{\text{g}} \neq 0$, the condition (23) can be rewritten as:

$$\frac{\partial \mu}{\partial \bar{I}}\left[\lambda_x x + \delta\lambda_{\text{g}}(\bar{I} - I_{\text{g}})\right] + \delta\lambda_{\text{g}}\mu = 0, \tag{26}$$

then replacing the definition of μ, leads to the following quadratic equation:

$$\left(\frac{\lambda_x x}{\delta\lambda_{\text{g}}} - I_{\text{g}}\right)\left(1 - \frac{k_d}{k_r}\tau(\sigma\bar{I})^2\right) + 2\bar{I} + \tau\sigma\bar{I}^2 = 0\,. \tag{27}$$

Candidate roots are of the form:

$$\bar{I}^* = \frac{-1 \pm \sqrt{1 - \tau\sigma\left(\frac{\lambda_x x}{\delta\lambda_{\text{g}}} - I_{\text{g}}\right) + \frac{k_d}{k_r}\tau\sigma^2\left(\frac{\lambda_x x}{\delta\lambda_{\text{g}}} - I_{\text{g}}\right)^2}}{\tau\sigma\left[1 - \frac{k_d}{k_r}\tau\sigma\left(\frac{\lambda_x x}{\delta\lambda_{\text{g}}} - I_{\text{g}}\right)\right]}, \tag{28}$$

of which only the positive roots are admissible.

Proposition 2. *For almost all $t \in [0, T_{\text{f}}]$, the optimal control I^* satisfies*

$$I^*(t) = \begin{cases} I_{\max} \text{ if } \bar{I}^* > \epsilon I_{\max}, \\ \bar{I}^*/\epsilon \text{ otherwise.} \end{cases} \tag{29}$$

with $\bar{I}^* > 0$ as in Eqn. (28).

The function Ψ, combined with the transversality conditions, is also useful to estimate the final arc of the optimal control D^*. From the terminal condition (14) and by continuity of λ_x, there is a time interval on which $\lambda_x(t) < 1$; it follows from Proposition 1 that $D(t) = D_{\max}$ on this interval.

To estimate the corresponding switching time T_{harv}, we rewrite the dynamic of the co-state λ_x as

$$\dot{\lambda}_x = -\Psi\frac{\partial \bar{I}}{\partial x} - \lambda_x(\mu - R - D) - D, \tag{30}$$

with Ψ as defined in (22) and noting the chain rule $\frac{\partial \mu}{\partial x} = \frac{\partial \mu}{\partial \bar{I}}\frac{\partial \bar{I}}{\partial x}$. Since $\frac{\partial \bar{I}}{\partial x} = I\frac{\partial \varepsilon}{\partial x}$ is non-positive (as more biomass decreases the average light in the photobioreactor), the condition (22) can be rewritten as:

$$\begin{aligned} \dot{\lambda}_x &\geq -\lambda_x(\mu - R - D) - D, \\ &\geq -\lambda_x(\mu_{\max} - R - D_{\max}) - D_{\max}. \end{aligned} \tag{31}$$

Multiplying both side by $e^{(\mu_{\max}-R-D_{\max})(t-(T_{\text{f}}-T_{\text{harv}}))}$ and integrating over time gives:

$$\begin{aligned} &\lambda_x(T_{\text{f}})e^{(\mu_{\max}-R-D_{\max})T_{\text{harv}}} \\ -\lambda_x(T_{\text{f}} - T_{\text{harv}}) \geq &\frac{-D_{\max}(e^{(\mu_{\max}-R-D_{\max})T_{\text{harv}}} - 1)}{\mu_{\max} - R - D_{\max}}, \end{aligned} \tag{32}$$

After replacing the transversality condition and $\lambda_x(T_{\text{f}} - T_{\text{harv}}) = 1$, we obtain:

$$\frac{\mu_{\max} - R}{D_{\max}} \geq e^{(\mu_{\max}-R-D_{\max})T_{\text{harv}}}. \tag{33}$$

We summarize this insight in Proposition 3 below.

Proposition 3 (Final harvest time)**.** *There exists $T_{\text{harv}} > 0$ such that $D^*(t) = D_{\max}$ for all $t \in [T_{\text{f}} - T_{\text{harv}}, T_{\text{f}}]$. If $\lambda_x(T - T_{\text{harv}}) = 1$, then*

$$T_{\text{harv}} \leq \frac{1}{\mu_{\max} - R - D_{\max}} \ln\left(\frac{\mu_{\max} - R}{D_{\max}}\right). \tag{34}$$

5. NUMERICAL INVESTIGATIONS

We solve the optimal control problem (OCP) using the direct sequential method, as implemented in the software BOCOP [Bonnans et al. 2017] with the NLP solver IPOPT [Wächter and Biegler 2006]. Figure 1 displays the results of the states and the controls with $I_{\max} = 1000$ µmol m^{-2}s^{-1}, $D_{\max} = 0.001$ s^{-1}, and $T_f = 20.8$ d together with the corresponding model parameter values.

The optimal dilution rate control in the numerical solution presents a clear *bang-singular-bang* structure, in agreement with Proposition 1. The optimal light irradiance control also comprises three main arcs. Along the first arc, the optimal dilution control remains at zero in order for the biomass to grow at maximal rate, while the optimal irradiance control is chosen to minimize the effect photoinhibition. Then, soon after the irradiance control has reached its maximum value $I_{\max}$, the singular arc of dilution stabilizes the biomass to a certain value that does not depend on the initial condition of the growth irradiance (see Fig 2). The final arc is activated around $t = T_{\text{f}} - T_{\text{harv}}$, in agreement with Proposition 3, where the optimal dilution control is set at its maximum value $D_{\max}$.

We refine the insight derived form the numerical solution below, with a focus on characterizing the optimal solution structure and approximating the optimal dilution rate

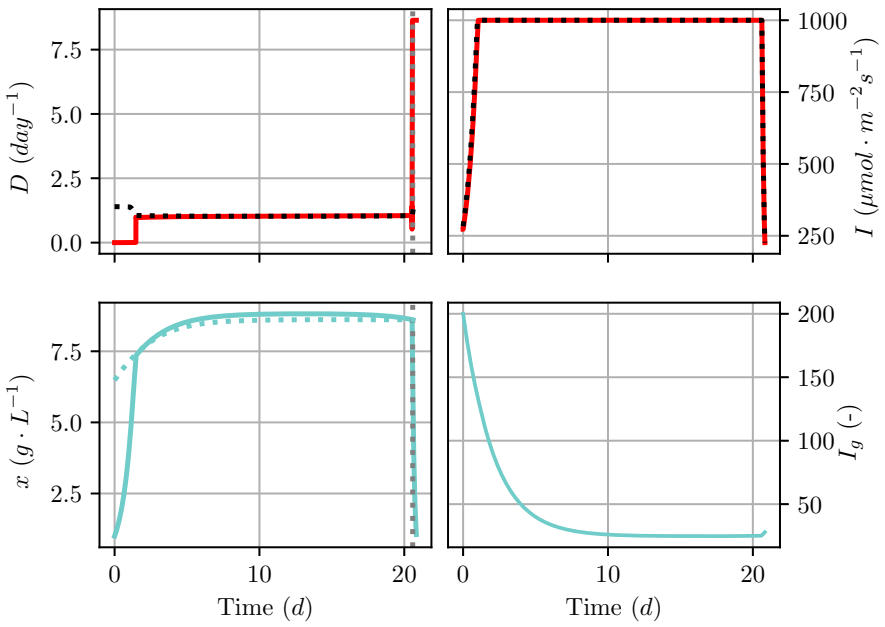

Parameter	Value
K	1.00×10^{-6} –
τ	5.50×10^{-3} s
k_d	5.00×10^{-6} –
k_r	1.50×10^{-4} s^{-1}
δ	2.30×10^{-1} –
ψ	3.10×10^{-1} $g_{Chl}\, g_C^{-1}$
k_I	4.40×10^{2} $\mu mol\, m^{-2} s^{-1}$
R	1.45×10^{-5} s^{-1}
E_c	8.00×10^{1} $g_C^{-1} m^{-1} L$
E_{chl}	4.00×10^{1} $g_{Chl}^{-1} m^{-1} L$
κ	1.00 –
β	5.48 (μmol, m, g)
L	5.00×10^{-2} m

Fig. 1. **Left:** Numerical solution with initial conditions $x(0) = 1$ and $I_g(0) = 200$. Red lines: optimal dilution rate and irradiance controls. Blue lines: optimal biomass concentration and growth irradiance states. Black dotted lines: value of $\mu - R$ (D plot) and approximate feedback control in Eqn. (39) (I plot). Vertical gray dotted lines: final harvest time T_{harv}. Blue dotted line: solution of Eqn. (40). **Right:** Model parameter values [Nikolaou et al. 2016].

along the singular arc and the optimal irradiance during the initial growth phase.

Since λ_x is a continuous function and according to Proposition 1, the optimal dilution rate profile is necessarily a concatenation of arcs, either $D^*(t) = 0$, $D^*(t) = D_{\max}$, or $D^*(t) = D_{\text{sing}}(t)$. Our computational investigations suggest that the structure of the optimal dilution rate follows a similar pattern presented in [Grognard et al. 2014, Theorem 2], where structures are possible for the optimal dilution rate:

(1) *Constant* control with $D^*(t) = D_{\max}$;
(2) *Bang-Bang* with $D^*(t) = 0$, and single switch to $D^*(t) = D_{\max}$;
(3) *Bang-Singular-Bang* with $D^*(t) = 0$ or $D^*(t) = D_{\max}$, a switch to $D(t) = D_{\text{sing}}(t)$, followed by a single switch to $D^*(t) = D_{\max}$.

The presence of the singular arc depends on the final time T_f, where the turnpike property appears; while the case $D^*(t) = 0$ or $D^*(t) = D_{\max}$ in the initial bang of the bang-singular-bang structure depends on the initial biomass concentration [Fierro U. et al. 2023]. Next, we focus on the more interesting case where T_f is large enough to trigger the singular arc and the initial biomass concentration is small enough for $D^*(t) = 0$ along the first arc. If the singular arc takes place in the interval $[t_1, t_2]$, then $\dot{\lambda}_x = 0$ for every $t \in (t_1, t_2)$ and, from (30), we have:

$$-\Psi \frac{\partial \bar{I}}{\partial x} = \mu - R. \tag{35}$$

Recalling that $\frac{\partial \bar{I}}{\partial x}$ is non-positive, and Ψ is also non-negative, we conclude that $\mu - R \geq 0$. Numerical simulations confirm that $\mu - R > 0$ and, consequently, $I^* = I_{\max}$ along the singular arc. We can always ensure that $I^* = I_{\max}$ along the singular arc by assuming the existence of a strictly positive lower bound $\underline{\mu}$ on the growth rate μ that satisfies

$$\underline{\mu} > R. \tag{36}$$

This condition is common in photobioreactor optimization [Masci et al. 2010, Bernard and Lu 2022], where it is assumed that microalgae keep growing when continuously exposed to light. This condition is not easy to establish, since it depends on the model parameters and on the choice of $I_{\max}$. However, we can notice that $I^* \neq I_{\max}$ only when $\mu = R$. This equation has two solutions when $R < \mu_{\max}$, one related to a photolimited condition and in a photoinhibited condition. If we rule out the case when this equality occurs in photoinhibition conditions (which imposes a condition over $I_{\max}$), then $I^* < I_{\max}$ does not fulfil the condition (15).

5.1 Approximate Feedback Control on Light Irradiance

Eqn. (26) can be rewritten as

$$\lambda_x x \frac{\partial \mu}{\partial \bar{I}} + \delta \lambda_g \left[\frac{\partial \mu}{\partial \bar{I}} (\bar{I} - I_g) + \mu \right] = 0. \tag{37}$$

Since δ is relatively small, the quantity $\delta \lambda_g$ itself is small enough to approximate its value to zero. We could confirm this through numerical simulations. Consequently, the optimal average irradiance $\bar{I}^*$ can be approximated using Eqn. (25), instead of the complex expression in Eqn. (28):

$$\bar{I}^*(t) \approx \frac{1}{\sigma \sqrt{\frac{k_d}{k_r} \tau}}, \tag{38}$$

whenever $\bar{I}^*(t) \leq \epsilon(x^*(t), I_g^*(t)) I_{\max}$. The optimal light irradiance control, therefore, can be approximated using the following closed-loop feedback control law:

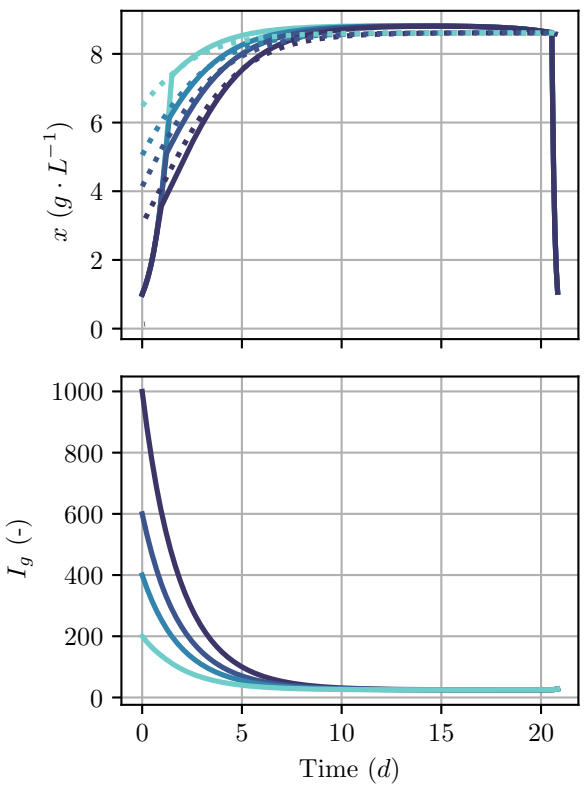

Fig. 2. Optimal trajectories for the initial concentration $x(0) = 1\ \mathrm{g\,L^{-1}}$ and different initial growth irradiance $I_{\mathrm{g}}(0) = 1000, 600, 400, 200\ \mu\mathrm{mol\,m^{-2}s^{-1}}$. The dotted lines represent the solution of the Eqn. (40), which correspond to the approximation of the optimal biomass.

$$I_{\mathrm{cl}}(x^*(t), I_{\mathrm{g}}^*(t)) := \min\left\{\frac{1}{\sigma(I_{\mathrm{g}}^*(t))\epsilon(x^*(t), I_{\mathrm{g}}^*(t))\sqrt{\frac{k_d}{k_r}\tau}}, I_{\max}\right\}. \quad (39)$$

Refer to Figure 1 for a comparison showing excellent agreement between the feedback control I_{cl} (black dotted line) and the numerically optimized I^* (red solid line). Also note that the optimal control in (29) converges pointwise to I_{cl} as δ approaches 0.

5.2 Approximate Optimal Biomass Concentration

Numerical simulations show that the biomass concentration x is constant along the singular arc, suggesting that the optimal dilution rate is adjusted to fulfill the condition $D_s = \mu - R$. Together with the approximation $\Psi \approx \lambda_x x \frac{\partial \mu}{\partial I}$ for sufficiently small δ, the optimal biomass concentration along the singular arc can then be approximated using (35) with $\lambda_x = 1$:

$$-x\frac{\partial \mu}{\partial x} \approx \mu - R. \quad (40)$$

This approximation matches the first-order optimality condition of the unrestricted, static problem $\max_x x(\mu - R)$ for a fixed I_{g} and $I = I_{\max}$. Refer to Figure 1 for a comparison between the solution to Eqn. (40) (dotted blue line) and the numerically optimized response x^* (solid blue line). Moreover, Figure 3 shows a plot of the net biomass productivity, defined by $(\mu(x, I_{\mathrm{g}}) - R)x$ for different biomass concentrations x and growth irradiance I_{g}. This phase diagram illustrates the turnpike property, whereby a range of optimal trajectories from different initial growth irradiance (blue solid lines) approach the maximal biomass concentration (black solid line), and ultimately the maximal net productivity. The same trajectories are shown in Figure 2 where, after the initial phase that is dependent on the initial conditions, the optimal dilution rate maintains a biomass density for which (at maximum irradiance) the average irradiance in the reactor leads to an optimal photoacclimation state and maximal growth rate.

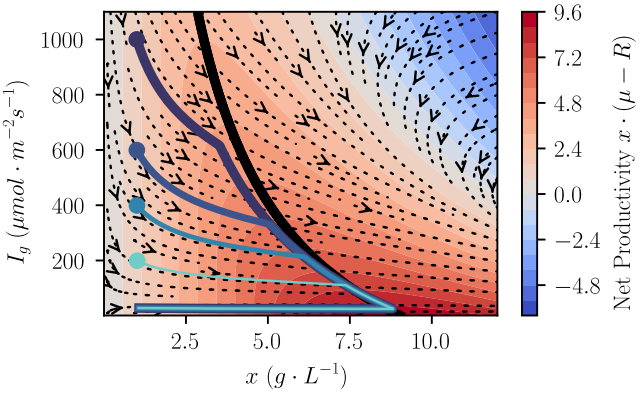

Fig. 3. Phase diagram of the net biomass productivity $(\mu(x, I_{\mathrm{g}}) - R)x$ and turnpike-like behavior. Dotted black lines: dynamic trajectories of biomass concentration x and growth irradiance I_{g} under the feedback control I_{cl}. Solid black line: maximal biomass concentration in terms of the growth irradiance I_{g}. Solid blue lines: selected trajectories from the initial biomass concentration $x(0) = 1\ \mathrm{g\,L^{-1}}$ and different initial growth irradiance $I_{\mathrm{g}}(0) = 1000, 600, 400, 200\ \mu\mathrm{mol\,m^{-2}s^{-1}}$.

6. DISCUSSIONS

6.1 On the Effect of Time Scales

Fierro U. et al. [2023] showed that the optimal dilution rate control D follows a turnpike strategy when considering the fast dynamics of photoinhibition in the growth model. Our results show that the turnpike property remains unchanged when accounting for the slower dynamics of photoacclimation. Upon combining the rapid protein damage and recovery dynamics with the gradual adaptation of pigments (photoacclimation), we can thus anticipate consistent results. In neither of these scenarios, however, are we in a position to formally establish the turnpike property, for instance using the results in Trélat and Zuazua [2015], due to the singularity of the Hessian matrix $\frac{\partial^2 H}{\partial D^2}$.

6.2 On Exploiting Self-Shading

One of the key features of the optimal strategy identified when accounting for both photoinhibition and photoac-

climation relies on exploiting self-shading to enhance the biomass growth by allowing the maximal light irradiance to be shone onto the photobioreactor. Typically, a small inoculum of microalgae is initially introduced into the photobioreactor. During the initial growth phase, the irradiance can be carefully adjusted to ensure that the average light intensity does not trigger significant photoinhibition. This initial phase of the optimal strategy cannot be applied in photobioreactors that use natural light, unless an external apparatus is used to dim light. Throughout this initial phase, the optimal dilution rate remains at zero. Then, once the optimal irradiance reach its maximum value and the optimal biomass level is attained, the optimal dilution rate is adjusted to keep this biomass concentration constant until the final harvesting time is reached.

7. CONCLUSIONS

We studied the optimal control problem of reactor startup considering photoinhibition, light gradient in the photobioreactor and photoacclimation dynamics, by combining a formal analysis with a numerical investigation. The rate of photoacclimation induces dynamics that are considerably slower than microalgal growth —as dictated by the time-scaling constant $\delta \ll 1$. This timescale difference translates into a magnitude difference in the co-states, in turn making it possible to formulate an approximate close-loop optimal control law for the light irradiance.

The optimal dilution rate presents a more challenging behavior for deriving a feedback control law, since it depends on the time horizon T_f. Nevertheless, its value can be approximated along the singular arc, which takes the values necessary to uphold optimal biomass levels to maximize net productivity.

Once the biomass is dense enough, self-shading enables operating the photobioreactor using the maximal irradiance to maximize biomass growth and the net productivity. This effect was previously studied, but only in the scenario where photoinhibition is negligible due to strong self-shading [Gerla et al. 2011]. Our analysis furthermore remains valid for average irradiance taking the form of $\bar{I} = \varepsilon I$, making the results transportable to other photobioreactor geometries such as tubular photobioreactors [Molina Grima et al. 1997, Grima et al. 1996].

REFERENCES

Bernard, O. and Lu, L.D. (2022). Optimal optical conditions for microalgal production in photobioreactors. *Journal of Process Control*, 112, 69–77.

Bernardi, A., Nikolaou, A., Meneghesso, A., Chachuat, B., Morosinotto, T., and Bezzo, F. (2017). Semi-empirical modeling of microalgae photosynthesis in different acclimation states – Application to N. gaditana. *Journal of Biotechnology*, 259, 63–72.

Blanken, W., Postma, P.R., de Winter, L., Wijffels, R.H., and Janssen, M. (2016). Predicting microalgae growth. *Algal Research*, 14, 28–38.

Bonnans, Frederic, J., Giorgi, D., Grelard, V., Heymann, B., Maindrault, S., Martinon, P., Tissot, O., and Liu, J. (2017). Bocop – A collection of examples. Technical report, INRIA.

Clarke, F. (2013). *Functional analysis, calculus of variations and optimal control*, volume 264. Springer.

Fierro U., J.I., Djema, W., and Bernard, O. (2023). Optimal control of microalgae culture accounting for photoinhibition and light attenuation. *IFAC-PapersOnLine*, 56(2), 7222–7227.

Fierro Ulloa, J.I., Lu, L.D., and Bernard, O. (2023). Theoretical growth rate of microalgae under high/low-flashing light. *Journal of Mathematical Biology*, 86(4), 48.

Gerla, D.J., Mooij, W.M., and Huisman, J. (2011). Photoinhibition and the assembly of light-limited phytoplankton communities. *Oikos*, 120(3), 359–368.

Grima, E.M., Sevilla, J.F., Pérez, J.S., and Camacho, F.G. (1996). A study on simultaneous photolimitation and photoinhibition in dense microalgal cultures taking into account incident and averaged irradiances. *Journal of Biotechnology*, 45(1), 59–69.

Grognard, F., Akhmetzhanov, A.R., and Bernard, O. (2014). Optimal strategies for biomass productivity maximization in a photobioreactor using natural light. *Automatica*, 50(2), 359–368.

Han, B.P. (2002). A mechanistic model of algal photoinhibition induced by photodamage to photosystem-II. *Journal of Theoretical Biology*, 214(4), 519–527.

Hartmann, P., Béchet, Q., and Bernard, O. (2014). The effect of photosynthesis time scales on microalgae productivity. *Bioprocess & Biosystems Engineering*, 37(1), 17–25.

Hocking, L.M. (1991). *Optimal control: an introduction to the theory with applications*. Oxford University Press.

Masci, P., Grognard, F., and Bernard, O. (2010). Microalgal biomass surface productivity optimization based on a photobioreactor model. *IFAC Proceedings Volumes*, 43(6), 180–185.

Molina Grima, E., García Camacho, F., Sánchez Pérez, J., Acién Fernández, F., and Fernández Sevilla, J. (1997). Evaluation of photosynthetic efficiency in microalgal cultures using averaged irradiance. *Enzyme and Microbial Technology*, 21(5), 375–381. doi:https://doi.org/10.1016/S0141-0229(97)00012-4.

Nikolaou, A., Hartmann, P., Sciandra, A., Chachuat, B., and Bernard, O. (2016). Dynamic coupling of photoacclimation and photoinhibition in a model of microalgae growth. *Journal of Theoretical Biology*, 390, 61–72.

Trélat, E. and Zuazua, E. (2015). The turnpike property in finite-dimensional nonlinear optimal control. *Journal of Differential Equations*, 258(1), 81–114.

Vázquez-Romero, B., Perales, J.A., Pereira, H., Barbosa, M., and Ruiz, J. (2022). Techno-economic assessment of microalgae production, harvesting and drying for food, feed, cosmetics, and agriculture. *Science of the Total Environment*, 837, 155742.

Wächter, A. and Biegler, L.T. (2006). On the implementation of an interior-point filter line-search algorithm for large-scale nonlinear programming. *Mathematical Programming*, 106(1), 25–57.